

# 1 **Cisplatin promotes pyroptosis of gastric cancer cells by activating GSDME**

2 Xianglai Jiang<sup>1, 2, 3#</sup>; Yongfeng Wang<sup>1, 2#</sup>; Chenyu Wang<sup>3</sup>; Haizhong Ma<sup>1, 2, 3</sup>; Miao Yu<sup>1, 2, 3</sup>; Hui

3 Cai<sup>1, 2, 3 \*</sup>

4 1 NHC Key Laboratory of Diagnosis and Therapy of Gastrointestinal Tumor, Gansu

5 Provincial Hospital, Lanzhou, lanzhou, 730000, China,

6 2 Gansu Provincial Hospital, Lanzhou, Lanzhou, 730000, China

7 3 Ningxia Medical University, Yinchuan, Yinchuan, 750004, China

8 # These authors contributed equally to this work.

9 \*\* Correspondence:

10 Hui Cai

11 caielonteam@163.com

## 12 **ABSTRACT**

13 According to studies, numerous chemotherapeutic drugs can facilitate programmed cell death  
14 via pyroptosis. Clarifying the mechanism by which cisplatin kills gastric cancer cells is  
15 crucial for enhancing gastric cancer's sensitivity to chemotherapy and elucidating the  
16 mechanism of drug resistance in gastric cancer. The differentially expressed genes following  
17 cisplatin treatment were identified using second-generation sequencing technology.  
18 Bioinformatics was used to investigate the functional enrichment of differentially expressed  
19 genes and core genes in tumor cells killed by cisplatin. Cox regression analyses were used to  
20 examine the pyroptosis core genes that worked as independent prognostic factors for patients  
21 with gastric cancer. The expression of core genes in gastric cancer cells was silenced by  
22 siRNA, and the changes in the proliferation of gastric cancer cells were observed. The  
23 expression of related genes and the survival of gastric cancer cells after the addition of  
24 cisplatin were observed. The second-generation sequencing, RT-PCR and Western blotting  
25 showed that the pyroptosis core gene was significantly highly expressed after cisplatin  
26 treatment. The results of differential gene enrichment of cisplatin-treated gastric cancer cells  
27 showed that differential genes were mainly concentrated in biological processes and signaling

**NOTE: This preprint reports new research that has not been certified by peer review and should not be used to guide clinical practice.**

28 pathways related to pyroptosis. GSDME protein is highly expressed after cisplatin treatment,  
29 and it is also a poor prognostic factor for gastric cancer patients and an independent  
30 prognostic factor. After the same dose of cisplatin treatment, the survival rate of siGSDME  
31 gastric cancer cells was significantly higher than that of GSDME regular expression gastric  
32 cancer cells. After acting on gastric cancer cells, cisplatin triggers pyroptosis by stimulating  
33 the activation of genes such as GSDME, resulting in the death of gastric cancer cells. GSDME  
34 is an independent prognostic factor for gastric cancer patients and is significantly linked with  
35 a shorter OS. In gastric cancer cells, silencing GSDME can substantially reduce cisplatin's  
36 cytotoxicity.

37 **Keywords:** *Cisplatin, Pyroptosis, GSDME, Chemotherapy*

### 38 **Introduction**

39 Gastric cancer is the fourth leading cause of cancer death (7.7 %), with more than  
40 700,000 deaths worldwide in 2020<sup>1-4</sup>. The origin of gastric cancer can be any part of the  
41 stomach and can spread to the whole stomach and even other organs (such as colorectal, liver  
42 and ovary)<sup>1</sup>. Gastric cancer is a disease with high molecular and phenotypic heterogeneity: in  
43 a multi-stage cascade process, gastritis caused by chronic *Helicobacter pylori* eventually  
44 develops into gastric cancer after precancerous stages of atrophic gastritis, intestinal  
45 metaplasia and dysplasia<sup>5</sup>. The mechanism of gastric cancer is complex and diverse, the  
46 biological processes involved include somatic mutation, mutation of proto-oncogenes and  
47 tumor suppressor genes, pyroptosis, apoptosis, and oxidative damage of DNA<sup>6</sup>. The initial  
48 symptoms of gastric cancer are not obvious, and clinical signs often manifest in the advanced  
49 stage of cancer<sup>7</sup>. When gastric cancer progresses to an unresectable stage, chemoradiotherapy  
50 is the main treatment<sup>8</sup>. In treating gastric cancer patients, the emergence of drug resistance  
51 and metastasis often means the failure of treatment. Therefore, it is significant to study the  
52 mechanism of gastric cancer chemotherapy and put forward new ideas to block the generation  
53 of drug resistance and improve sensitivity.<sup>9,10</sup>

54 Cells are the basic unit of life activities, and cell death, as a natural life phenomenon, is  
55 significant for maintaining the relative stability of the body's internal environment of the  
56 body<sup>11</sup>. Pyroptosis and apoptosis are both programmed cell death, and apoptosis will shrink  
57 into apoptotic bodies and be swallowed by phagocytes, so it does not cause inflammatory  
58 response<sup>12</sup>. The concept of pyroptosis was first proposed by Cookson and Brennan in 2001 to  
59 describe a cysteine protease 1 (CASP1) -dependent cell death in inflammatory cells<sup>13</sup>. Cells  
60 undergoing pyroptosis continue to expand until the cell membrane ruptures, leading to the

61 release of intracellular substances and the activation of a robust inflammatory response<sup>14</sup>.  
62 Pyroptosis is an indispensable natural immune response mediated by Gasdermin protein in the  
63 human body<sup>14</sup>. After receiving inflammatory stimulation, caspase family proteins cut  
64 Gasdermin protein and cause the cut Gasdermin protein to aggregate on the surface of the cell  
65 membrane to form a cavity, to achieve the role of cell content material outflow and cell  
66 death<sup>15</sup>. As an essential protective mechanism of human body, pyroptosis can timely remove  
67 infected or mutated abnormal cells and the presence of pyroptosis has an important anti-tumor  
68 effect<sup>16</sup>. Cisplatin is a platinum-containing anticancer drug. It is an orange or yellow  
69 crystalline powder, slightly soluble in water, easily soluble in dimethylformamide, and can be  
70 gradually converted and hydrolyzed in an aqueous solution<sup>17, 18</sup>. Clinical use of cisplatin in  
71 ovarian cancer, prostate cancer, testicular cancer, lung cancer, nasopharyngeal carcinoma,  
72 esophageal cancer, malignant lymphoma, head and neck squamous cell carcinoma, thyroid  
73 cancer and osteosarcoma and other solid tumors can show efficacy<sup>19, 20</sup>. Recent studies have  
74 shown that cisplatin can activate pyroptosis to mediate gastric cancer cells after acting on  
75 cancer cells, which has a new direction for the mechanism of cisplatin as a chemotherapeutic  
76 drug to kill gastric cancer cells<sup>21-23</sup>.

77 In this study, basic experimental techniques and bioinformatics analysis methods were  
78 used to identify the significantly differentially expressed apoptosis core genes and pyroptosis  
79 core genes after cisplatin treatment of gastric cancer cells. The expression of GSDME, a  
80 highly expressed pyroptosis execution factor after cisplatin treatment, in gastric cancer and its  
81 effect on the biological function of gastric cancer cells were explored. Finally, it was  
82 confirmed that silencing the expression of GSDME in gastric cancer cells reduced the  
83 sensitivity of gastric cancer cells to cisplatin, which proved that cisplatin mediated pyroptosis  
84 of gastric cancer cells by activating GSDME. It was found that GSDME was an independent  
85 prognostic factor for gastric cancer patients, and could potentially be a prognostic marker,  
86 chemotherapeutic drug sensitivity and immunotherapy biomarker.

## 87 **Material and method**

### 88 **2.1 Cell culture**

89 Human gastric epithelial cell (GES-1), human gastric adenocarcinoma cell (AGS) and human  
90 poorly differentiated gastric cancer cell (MKN45) were purchased from the Cell Resource  
91 Center of Shanghai Academy of Sciences. The cells were cultured in 4ml RPMI-1640  
92 medium containing 10 % fetal bovine serum (Biological Industries, Israel) and placed in a  
93 37 °C constant temperature cell incubator containing 5 % CO<sub>2</sub>. All cells were subcultures

94 when the growth length reached 80 %, and all cell lines maintained the typical morphology of  
95 the cells during the study.

## 96 **2.2 Determination of semi-inhibitory concentration**

97 AGS cells and MKN45 cells without abnormal morphology and growth status were obtained.  
98 After the cells reached the preset concentration and were in the logarithmic phase of growth  
99 observed by the microscope, cisplatin (APEXBIO, USA) of 0 $\mu$ M, 5 $\mu$ M, 12.5 $\mu$ M, 25 $\mu$ M,  
100 50 $\mu$ M and 100 $\mu$ M were added respectively, and the cells were transferred to 37 °C and 5 %  
101 CO<sub>2</sub> cell incubator for 12 h. After 12 hours of culture, 100ul of the mixture was gently  
102 removed and 10ul of CCK8 reagent (APEXBIO, USA) and 100ul of serum-free medium  
103 (Biological Industries, Israel) were added. The cells were cultured in a 37 °C thermostatic  
104 shaker for 1 hour, and then the OD value of each well was measured at a wavelength of 450  
105 nm on a microplate reader (Thermo Scientific, USA). The measured OD value was converted  
106 into a percentage value to obtain the drug concentration and the corresponding inhibition rate  
107 and imported into EXCEL software and GraphPad Prism 8.0 software. The IC<sub>50</sub> of cisplatin  
108 on gastric cancer cells AGS and MKN45 for 12 hours was calculated and the corresponding  
109 figures were drawn.

## 110 **2.3 The second-generation sequencing detection**

111 MKN45 cells were treated with IC<sub>50</sub> cisplatin, and the total RNA of MKN45 cells was  
112 extracted by Invitrogen TRIzol as the initial input material. The initial input material is  
113 enzymatically shredded to conform to the fragments required by the Illumina machine. The  
114 single-stranded DNA fragment in the sample was entered into the flow cell and then  
115 combined with the P5 ' of the flow cell to complete the bridge PCR amplification. A special  
116 dNTP with four different fluorescent groups was added to emit different fluorescence signals  
117 at the same time, and then the extension-scanning process was repeated until the entire DNA  
118 sequence was spliced. The differentially expressed mRNAs before and after gastric cancer  
119 cell MKN45 were sequenced using the principle of reversible termination of chemical  
120 reactions through four special deoxyribonucleotides that can emit fluorescence signals.

## 121 **2.4 Real-time fluorescent quantitative PCR**

122 The total RNA of 10 pairs of gastric cancer clinical samples was extracted strictly according  
123 to the manufacturer's requirements. The extracted RNA was reverse transcribed into cDNA  
124 using a reverse transcription kit (vazyme, China), and the reaction system was configured  
125 according to 10ul SYBR green reagent, 7.2ul DEPC water, 2ul cDNA, 0.4ul pre-primer and  
126 0.4ul post-primer. According to the pre-deformation: 95 °C / 5 minutes (one cycle) ; cyclic

127 reaction : 95 °C / 10s-60 °C / 30s (40 cycles) ; dissolution : 95 °C / 15s-60 °C / 60s-95 °C /  
128 15s (one cycle) reaction procedure for PCR quantification. The quantitative fluorescence  
129 analysis of GSDME with GAPDH as the internal reference gene was completed under the  
130 lighter machine (Roche, Switzerland). The expression of GSDME in different tissues was  
131 calculated according to the  $2^{-\Delta\Delta CT}$  method, the statistical analysis was completed in GraphPad  
132 Prism 8.0 software, and the corresponding patterns were drawn.

### 133 Primers Sequences

Name	Sequence (5'-3')	Segment length (bp)	Annealing (°C)
GSDME	F: TACTTCTTGGTCAGTGCCCTCG	174	61.98
	R: CCTTTCTGTATCTTTCAGGGGAGT		59.77
GAPDH	F: GGAAGCTTGTCATCAATGGAAATC	168	62.4
	R: TGATGACCCTTTTGGCTCCC		62

### 134 2.5 Western blot detection

135 The treated GES-1, AGS and MKN45, as well as MKN45 and AGS co-cultured with cisplatin  
136 for 24 h were taken out in an incubator at 37 °C, and the proteins were extracted and  
137 quantified. The protein separated by electrophoresis was transferred to the PVDF membrane,  
138 quickly blocked for 30 minutes, then placed in a specific primary antibody (abcam, UK) and  
139 incubated in a 4 % environment for 12 hours. Then the anti-rabbit antibody (proteintech,  
140 China) was incubated at room temperature for 2 hours, and the gel imaging system (eBlot,  
141 China) was used for imaging after using the chromogenic agent.

### 142 2.6 mRNA data collection

143 The RNA-Seq expression profile data of TCGA-STAD were obtained by logging into the  
144 TCGA database website (<https://www.cancer.gov/>) in December 2022. At the same time, the  
145 expression profiles of cancer tissues and adjacent tissues of gastric cancer patients and the  
146 clinical information of gastric cancer patients were collected from the TCGA database. The  
147 expression of core genes in gastric cancer was analyzed using the GEPIA 2 website  
148 (<http://gepia2.cancer-pku.cn/>) in December 2022<sup>24</sup>. The immunohistochemical images of core  
149 gene protein expression in 'stomach' and 'gastric cancer' were downloaded from the human  
150 protein atlas (<https://www.proteinatlas.org>) database in January 2023.

### 151 2.7 Single-factor regression analysis

152 To prepare the correlation expression of core genes in stomach adenocarcinoma (STAD)  
153 samples in each TCGA database and the corresponding survival status and survival time  
154 matrix, as well as the matrix that converts clinical information (age, gender, grade, stage

155 staging, T staging, M staging and N staging) into continuous variables. The prepared matrix  
156 information was input, and the ' bioForest ' function and ' indep ' function in the ' survival '  
157 software package in R software were applied to complete the single factor Cox regression  
158 analysis of core genes for gastric cancer patients to explore whether core genes can be used as  
159 independent prognostic factors for gastric cancer patients. The expression data of ten  
160 pyroptosis-related genes CASP1, CASP8, CHMP6, GSDMD, GSDME, IL6, NCRC5, NLRP1,  
161 NLRP6 and TP53 highly expressed after cisplatin stimulation were selected as continuous  
162 variables in the Cox regression model for analysis.

### 163 **2.8 Ethics**

164 This study was approved by the Medical Ethics Association of Gansu Provincial People 's  
165 Hospital, ethical number: 2022316. All patients signed the informed consent form and agreed  
166 to the study, and all processes were in line with the Declaration of Herkissin. After the patient  
167 's family members and patients have been informed and obtained their permission, the  
168 abandoned cancer tissues and adjacent tissues of patients who underwent gastric cancer  
169 resection in Gansu Provincial People 's Hospital from August 28, 2022 - September 30, 2022  
170 were collected, which conforms to the principle of controlling risks and protecting the safety  
171 and health rights of subjects. RNA was extracted from discarded tumor tissues and adjacent  
172 tissues and stored in a refrigerator at -80 °C. The information of all subjects was strictly  
173 confidential, and the relevant information was not disclosed to any third party without the  
174 authorization of the subject, in line with the principle of privacy protection.

### 175 **2.9 Gene enrichment analysis**

176 The analysis included different genes with p values less than 0.05 before and after cisplatin  
177 treatment. Gene ontology (GO) and Kyoto Encyclopedia of Genes and Genomes (KEGG)  
178 enrichment analysis were performed on the differential gene set using the 'org.Hs.eg.db 'R  
179 software package<sup>25</sup>. According to the expression level of gastric cancer patients in the TCGA  
180 database, they were divided into two groups, and the differentially expressed genes in the core  
181 gene high expression group and the core gene low expression group were identified. The  
182 differential genes of the two groups of core genes were analyzed by GO and KEGG  
183 enrichment analysis.

### 184 **2.10 Kaplan-Meier survival analysis**

185 According to the median value of core gene expression, gastric cancer patients in the TCGA  
186 database were divided into high core and low core gene expression groups. The comparison of  
187 OS between the two groups with high core gene expression can be completed, and the

188 correlation between core gene expression and survival time of gastric cancer patients can be  
189 explored<sup>26</sup>. The 'limma' R software package, 'survival' R software package and 'survminer'  
190 R software package were used to calculate the correlation between core gene expression and  
191 survival time and survival status of patients, and to explore the correlation between core gene  
192 expression and overall survival (OS), progression-free survival (FP) and post-progression  
193 survival (PPS) of patients with gastric adenocarcinoma.

#### 194 **2.11 Tumor microenvironment analysis**

195 The "Estimate" R software package was used to complete the scoring of each gastric cancer  
196 sample in the TCGA database. The gastric cancer samples were divided into core gene high  
197 expression group and core gene low expression group according to the expression of core  
198 genes. StromalScore, ImmuneScore and ESTIMATEScore determined the effect of core gene  
199 expression on tumor microenvironment.

#### 200 **2.12 Tumor immune cell infiltration analysis**

201 The 'CIBERSORT' R package was used to calculate the degree of immune cell infiltration in  
202 each sample and to analyze the correlation between the expression of core genes and the  
203 degree of immune cell infiltration.

#### 204 **2.13 Immune checkpoint inhibitor expression analysis**

205 The expression information of CD40, NRP1, TNFSF4, TNFRSF8, CD86, TNFRSF25,  
206 TNFRSF4, VTCN1, CD28, TNFSF18, TNFSF15, CD200, PDCD1LG2, LGALS9, TNFSF9,  
207 LAIR1, TNFSF14, ADORA2A and CD276 in gastric cancer was obtained, and the correlation  
208 between the expression of these immune checkpoint inhibitor genes and the core expression  
209 was analyzed.

#### 210 **2.14 Correlation analysis of tumor mutation burden**

211 Tumor mutation burden (TMB) refers to the total number of somatic gene coding errors, base  
212 substitutions, gene insertions or deletion errors (mut / Mb) detected per million bases. High  
213 TMB tumor cells help anti-tumor T cell proliferation and anti-tumor response. It is currently  
214 an FDA-certified immunotherapy biomarker<sup>27</sup>. The TMB data of gastric cancer samples in  
215 TCGA database were obtained, and the correlation between core gene expression and TMB  
216 was calculated.

#### 217 **2.15 Correlation between core gene expression and IPS**

218 Immunophenoscore (IPS), as an indicator of tumor immunogenicity, can predict the effect of  
219 immunotherapy in cancer patients<sup>28</sup>. Immunotherapy data were obtained from The Cancer  
220 Immunome Atlas (<https://tcia.at/home>) to analyze the correlation between the expression of

221 core genes and IPS treated with CTLA4 (-) PD1 (-), CTLA4 (-) PD1 (+), CTLA4 (+) PD1 (-)  
222 and CTLA4 (+) PD1 (+) in January 2023.

### 223 **2.16 Small interfering RNA silencing core gene expression**

224 The gastric cancer cells AGS and MKN45 were cultured in a 37 °C constant temperature cell  
225 incubator. In strict accordance with the instructions, 300,000 cells and six-well plates were  
226 inoculated respectively and cultured for 24 hours to make them fully adherent. When the cell  
227 concentration reached 80 %, it was taken out from the cell incubator. The siRNA was diluted  
228 according to the ratio of 50 ul Opti-MEM medium, 250 pmol siRNA and 12.5 ul TransIntro @  
229 EL transfection reagent, and the siRNA-TransIntro @ EL complex was prepared by gently  
230 blowing and mixing. After 20 minutes at room temperature, the siRNA-TransIntro @ EL  
231 complex was added to a six-well plate with a cell density of 80 %. The cells were cultured in  
232 a 37 °C / 5 % constant temperature cell incubator. After 4 hours, the medium was replaced to  
233 improve the transfection efficiency. The transfection efficiency was observed by fluorescence  
234 microscopy at 24 hours and 48 hours. The cell protein was extracted, and the expression of  
235 the target protein was detected to further confirm the transfection efficiency, to select the  
236 siRNA with the highest transfection efficiency.

### 237 **2.17 Statistics**

238 Student *t* test was performed on two sets of data with normal distribution and homogeneity of  
239 variance, *t'* test was performed on data with normal distribution and heterogeneity of variance,  
240 and Mann-Whitney test was used for data that did not conform to normal distribution. The  
241 limma algorithm was used to calculate the differential genes in the transcriptome. The  
242 correlation between the expression of the target gene and the tumor microenvironment score  
243 was analyzed by Wilcox test. The correlation between the target gene and immune cell  
244 infiltration, immune checkpoint inhibitor gene expression and tumor mutation load was  
245 analyzed by Spearman test.

## 246 **Results**

### 247 **1 Viability curve of gastric cancer cells**

248 CCK8 analysis showed that the growth of AGS cells and MKN45 cells was significantly  
249 inhibited after treatment with 0μM, 5μM, 12.5μM, 25μM, 50μM and 100μM cisplatin for 12  
250 hours (Fig.1.A-B) and 24 hours (Fig.1.C-D). The IC<sub>50</sub> value of AGS cells treated with  
251 cisplatin for 12 hours was 8.147μM. The IC<sub>50</sub> value of MKN45 cells was 8.660μM.

### 252 **2 Identification of differential genes**

253 The second-generation sequencing results showed that 9978 genes were significantly



254 differentially expressed after MKN45 cells were treated with cisplatin 8.660  $\mu$ M (IC50).  
255 Among them, 10 pyroptosis core genes NLRP6 (logFC = 3.270586096, p = 0.000708546),  
256 IL6 (logFC = 1.646344676, p = 0.000325408), GSDME (logFC = 0.666460514, p =  
257 1.47581E-06), NLRP1 (logFC = 2.19681335, p = 9.2746E-15), CHMP6 (logFC =  
258 1.27873683, p = 1.55749E-07), GSDMD (logFC = 0.742823512, p = 0.000133279), NLRC5  
259 (logFC = 1.246191075, p = 1.20937E-19), TP53 (logFC = 1.860FC503494, p =  
260 2.3254E-0.74823). Two genes CASP3 (logFC = - 2.226428178, p = 1.27397E-75) and  
261 TNFRSF10B (logFC = - 0.602568568, p = 1.25251E-07) were significantly decreased after  
262 cisplatin stimulation (Fig.2.A).

### 263 **3 Gene enrichment analysis**

264 GO enrichment analysis of differential genes before and after cisplatin treatment of MKN45  
265 showed that differential genes were mainly concentrated in biological processes such as  
266 positive regulation of catabolic process, proteasome protein catabolic process and ncRNA  
267 metabolic process. Differential genes were mainly concentrated in cell component such as  
268 mitochondrial inner membrane, cell-substrate junction and focal adhesion. Differential genes  
269 were mainly concentrated in molecular function such as transcription coregulatory activity,  
270 DNA-binding transcription factor binding and catalytic activity, acting on RNA. Differential  
271 genes were mainly concentrated in pathways such as pathway of neurodegeneration-multiple  
272 diseases, Alzheimer disease, and Amyotrophic lateral sclerosis (Fig.2.B).

### 273 **4 Cox regression analysis**

274 The above ten pyroptosis genes significantly increased in MKN45 cells after 12 h of IC50  
275 cisplatin stimulation were used to explore the effect of these ten genes on the overall survival  
276 of gastric cancer patients using Cox regression model. The results showed that GSDME was  
277 an independent prognostic factor for gastric cancer patients (Fig.3.A). CASP1, CASP8,  
278 CHMP6, GSDMD, IL6, NLRC5, NLRP1, NLRP6 and TP53 are not independent prognostic  
279 factors for gastric cancer patients (Fig.3.B-J).

### 280 **5 Related changes after cisplatin treatment of gastric cancer cells**

281 Western blot was used to detect the expression of GSDME protein (p = 0.0096), B-Cell CLL /  
282 Lymphoma 2 (Bcl-2) protein (p = 0.0124) and Caspase-3 (CASP3) protein (p = 0.0032) in  
283 human gastric adenocarcinoma AGS cells after cisplatin stimulation. The expression of  
284 GSDMD protein (p = 0.0455) was significantly decreased. There was no significant difference  
285 in the expression of Poly (ADP-Ribose) Polymerase (PARP) protein and Interleukin-1beta  
286 (IL-1 beta) protein. The expression of GSDME protein (p = 0.0047) and Bcl-2 protein (p =

287 0.0217) in human gastric cancer cell MKN45 showed a significant high expression trend, and  
288 the expression of GSDMD protein ( $p = 0.0061$ ) also showed a significant decrease, while the  
289 expression of CASP3, PARP protein and IL-1 beta protein was not significantly different  
290 (Figure 5.A-C).

## 291 **6 Expression of GSDME in gastric cancer**

292 The results showed that the expression of GSDME in gastric cancer tissues and adjacent  
293 tissues was statistically different ( $p = 0.0239$ ), but the expression difference logFC was 0.3  
294 (Fig.5.A). According to the results of qRT-PCR analysis, there was no significant difference in  
295 the expression of GSDME in 10 pairs of gastric cancer tissues and adjacent tissues (Fig.5.B).  
296 Western Blot analysis showed that compared with the expression of GSDME protein in  
297 gastric epithelial cells GES-1, there was no difference in the expression of human gastric  
298 adenocarcinoma cells AGS, but lower expression in MKN45 cells (Figure.5.C-D).  
299 Immunohistochemical images of GSDME in gastric cancer patients were collected from the  
300 human protein atlas database. The results showed that the expression of GSDME protein in  
301 gastric cancer tissues and adjacent tissues was mainly 'medium' intensity (Fig.5.E-F).

## 302 **7 Prognostic analysis**

303 KM prognostic analysis showed that high expression of GSDME (DFNA5) was significantly  
304 associated with shorter OS in gastric cancer patients ( $p = 1.6e - 06$ , HR : 1.53 (1.28 - 1.82),  
305 Fig.6.A), and high expression of GSDME was significantly associated with shorter FP in  
306 gastric cancer patients ( $p = 1.7e - 05$ , HR : 1.55 (1.27 - 1.89), Fig.6.B). High GSDME  
307 expression was significantly associated with shorter PPS in gastric cancer patients ( $p =$   
308  $0.00016$ , HR : 1.52 (1.22 - 1.9), Fig.6.C).

## 309 **8 Correlation between GSDME and clinical characteristics of gastric cancer patients**

310 The clinical analysis results showed that GSDME was highly expressed in gastric cancer  
311 patients less than or equal to 65 years old compared with patients older than 65 years old  
312 (Fig.6.D). Compared with Stage I stage, GSDME was higher expressed in Stage II patients  
313 (Fig.6.G) ; compared with T1 stage, GSDME had higher expression in T4 patients (Fig.7.H).  
314 There was no significant difference in the expression of GSDME in gastric cancer patients  
315 with different genders (Fig.6.E), different Grades (Fig.6.F), different N stages (Fig.6.I) and  
316 different M stages (Fig.6.J).

## 317 **10 Correlation between GSDME expression and tumor microenvironment score**

318 The results of immune microenvironment analysis showed that the expression of GSDME  
319 was significantly positively correlated with StromalScore, ImmuneScore and

320 ESTIMATEScore (Fig.7.A).

### 321 **11 Correlation between GSDME expression and immune cell infiltration**

322 The immune cell infiltration analysis results showed that the expression of GSDME was  
323 significantly positively correlated with Macrophage M1 and T cells CD4 memory activated  
324 (Fig.7.B).

### 325 **12 Correlation between GSDME expression and immune checkpoint inhibitor 326 expression**

327 In gastric cancer, the expression of GSDME was positively correlated with the expression of  
328 CD40, NRP1, TNFSF4, TNFRSF8, CD86, TNFRSF25, TNFRSF4, VTCN1, CD28, TNFSF18,  
329 TNFSF15, CD200, PDCD1LG2, LAIR1, TNFSF14, ADORA2A and CD276, but negatively  
330 correlated with the expression of LGALS9 and TNFSF9 (Fig.7.C).

### 331 **13 Correlation between GSDME expression and TMB**

332 TMB analysis showed that GSDME expression was significantly negatively correlated with  
333 tumor mutation burden in gastric cancer (Fig.7.D).

### 334 **14 Correlation between GSDME expression and IPS**

335 Immunotherapy analysis showed that the expression of GSDME was significantly negatively  
336 correlated with IPS in patients (Fig.7.E-H) with gastric cancer treated with CTLA4 (+) PD 1  
337 (+), CTLA4 (+) PD 1 (-) and CTLA4 (-) PD 1 (+).

### 338 **15 Changes after transfection of siRNA GSDME**

339 Compared with NC siRNA treatment, AGS cell treated with GSDME small interfering RNA  
340 had significantly better proliferation ability at 12 hours ( $p = 0.0031$ ) and 24 hours ( $p = 0.0104$ )  
341 after gastric cancer cells were treated with GSDME small interfering RNA (Fig.8.A) ;  
342 MKN45 cell had significantly worse proliferation ability at 24 hours ( $p < 0.0001$ ) and 48  
343 hours ( $p = 0.0339$ ) (Fig.8.B). The results of Western Blot experiments and analysis showed  
344 that after GSDME expression was silenced, the expression of PARP protein ( $p = 0.0259$ ) and  
345 Bcl-2 protein ( $p = 0.0022$ ) in human gastric adenocarcinoma AGS cell decreased significantly,  
346 while the expression of CASP3 protein ( $p = 0.0239$ ) increased significantly, and the  
347 expression of GSDMD protein ( $p = 0.7022$ ) and IL-1 beta protein ( $p = 0.6126$ ) did not change  
348 significantly. The expression of Bcl-2 protein ( $p = 0.0353$ ) was significantly decreased in  
349 human gastric cancer cell line MKN45, while the expression of CASP3 protein ( $p = 0.0136$ )  
350 was significantly increased. The expression of PARP protein ( $p = 0.1922$ ), GSDMD protein ( $p$   
351  $= 0.3427$ ) and IL-1 beta protein ( $p = 0.7945$ ) did not change significantly (Fig.8.C-E).

### 352 **16 The effect of GSDME expression on cisplatin cytotoxicity**

353 CCK8 results analysis showed that when the expression of GSDME in AGS cells and MKN45  
354 cells was silenced by siRNA, the cytotoxicity of cisplatin at 12 h was significantly reduced,  
355 and the survival rate of AGS cells ( $p < 0.001$ ) and MKN45 ( $p < 0.001$ ) cells treated with  
356 cisplatin at 12 h IC50 was significantly increased (Fig.9.A). Western Blot results showed that  
357 after cisplatin treatment of gastric cancer cells with IC50 concentration, compared with NC  
358 siRNA gastric cancer cells, in addition to the low expression of GSDME protein in AGS cells  
359 of siGSDME, GSDMD protein ( $p = 0.0034$ ), IL-1 beta protein ( $p = 0.0024$ ) and Bcl-2 protein  
360 ( $p = 0.0468$ ) showed significantly low expression, CASP3 protein ( $p = 0.0020$ ) showed  
361 significantly high expression; in addition to the low expression of GSDME protein in  
362 siGSDME MKN45 cells, GSDMD protein ( $p = 0.0099$ ), IL-1 beta protein ( $p = 0.0002$ ) and  
363 Bcl-2 protein ( $p = 0.0102$ ) showed significantly low expression, while CASP3 protein ( $p =$   
364  $0.0256$ ) showed significantly high expression (Fig.9.B-D).

## 365 **Discussion**

366 Cisplatin is widely used in chemotherapy for cancer, germ cell tumors, lymphoma and  
367 sarcoma. The traditional view is that cisplatin interacts with purine bases and interferes with  
368 intracellular DNA repair, resulting in irreparable DNA damage, which mediates apoptosis. In  
369 this study, the second-generation sequencing results showed that most apoptotic core genes  
370 did not show significant high expression after cisplatin treatment of human gastric cancer cell  
371 MKN45. Pyroptosis-related genes (NLRP6, IL6, GSDME, NLRP1, GSDMD, NLRC5,  
372 CASP8 and CASP1) showed a significant high expression trend after cisplatin treatment,  
373 indicating that cisplatin may promote the death of gastric cancer cells by activating pyroptosis.  
374 In 2001, Souza et al. first proposed the term ' pyroptosis ' to distinguish between apoptosis and  
375 pyroptosis, which belong to programmed cell death<sup>29</sup>. The study of shao et al. showed that  
376 GSDME was specifically cleaved by CASP3 in the adaptor under the action of  
377 chemotherapeutic drugs, resulting in GSDME-N fragment, which eventually led to pyroptosis  
378 of cancer cells expressing GSDME<sup>15</sup>. Cisplatin can activate pyroptosis through the MEG3 /  
379 NLRP3 / caspase-1 / GSDMD pathway to exert anti-tumor effects in triple-negative breast  
380 cancer<sup>21</sup>. Similarly, cisplatin can also mediate pyroptosis in esophageal cancer cells and lung  
381 cancer cells<sup>23, 30</sup>. In this study, the enrichment analysis of differential genes before and after  
382 cisplatin treatment showed that the differential genes were mainly concentrated in  
383 neurodegenerative diseases, amyotrophic lateral sclerosis, Alzheimer 's disease, Parkinson 's  
384 disease, human papillomavirus infection and shigellosis. Current research has found that  
385 abnormal activation of programmed cell death, including pyroptosis, leads to unnecessary loss

386 of neuronal cells and functions, which is one of the main characteristics of neurodegenerative  
387 diseases such as amyotrophic lateral sclerosis, Alzheimer 's disease, Parkinson 's disease and  
388 Huntington 's disease<sup>31, 32</sup>. Pyroptosis is closely related to Alzheimer 's disease. The activation  
389 of inflammasome can promote the accumulation of amyloid protein and the deterioration of  
390 neuronal function in APP / PS1 mice, leading to the onset of Alzheimer 's disease<sup>33</sup>. Using  
391 drugs to target the occurrence of pyroptosis mediated by NLRP3 inflammasome can improve  
392 the condition of Alzheimer 's disease and Parkinson 's disease<sup>34, 35</sup>. Shigella is the pathogen of  
393 bacillary dysentery. There is a clear relationship between Shigella and the occurrence of  
394 pyroptosis. It can inhibit the activation of inflammasomes in epithelial cells, optimize the  
395 interaction with the host and establish a successful infection by regulating the 'open' and  
396 'close' of inflammasomes<sup>36</sup>. The differential genes after cisplatin treatment of gastric cancer  
397 cells are concentrated in the signaling pathways of pyroptosis-related diseases, which also  
398 shows that there may be a strong correlation between cisplatin and pyroptosis.

399 The second-generation sequencing results showed that GSDME was significantly highly  
400 expressed after cisplatin treatment of cancer cells, and Western Blot also showed that GSDME  
401 protein was significantly highly expressed after cisplatin treatment of gastric cancer cells.  
402 GSDME protein is an independent prognostic factor in patients with gastric cancer, and  
403 previous studies have also shown that GSDME protein is an executive protein of  
404 chemotherapeutic drug-mediated pyroptosis<sup>37</sup>. Therefore, GSDME was selected as the core  
405 gene of cisplatin acting on gastric cancer cells for further analysis. The results of prognostic  
406 analysis showed that the high expression of GSDME was a risk factor for gastric cancer  
407 patients, which was significantly correlated with shorter OS, FP and PPS in gastric cancer  
408 patients. GSDME has the potential to be a prognostic marker for gastric cancer. Studies have  
409 shown that prediction models constructed using pyroptosis-related genes have good predictive  
410 performance in the diagnosis or prognosis of gastric cancer or immunotherapy<sup>38-41</sup>. Through  
411 KEGG enrichment analysis based on GESA, it was found that GSDME was negatively  
412 correlated with signal pathways such as aminoacyl-tRNA biosynthesis, DNA replication and  
413 nucleotide excision repair in gastric cancer. GSDME may inhibit DNA repair behavior in  
414 gastric cancer, which is also consistent with the related cognition of pyroptosis-mediated  
415 cancer cell death. Pyroptosis is a double-edged sword for tumor. The relationship between  
416 pyroptosis and tumor environment exists in various ways: it can kill cancer cells and promote  
417 inflammation to affect the formation and development of tumor<sup>42, 43</sup>. After silencing GSDME  
418 with siRNA, different cells showed different growth and proliferation. GSDME-silenced AGS

419 cells showed stronger proliferation ability after 12 hours and 24 hours of culture, while  
420 GSDME-silenced MKN45 cells showed worse proliferation ability after 24 hours and 48  
421 hours of culture. However, after 72 hours GSDME-silenced AGS cells and MKN45 cells  
422 showed the same proliferation ability as NC group AGS cells and MKN45 cells. Cells with  
423 different proliferation ability previously showed the same proliferation ability after 72 hours,  
424 which may be due to the timeliness of siRNA. However, other studies have also shown that  
425 GSDME may not be directly involved in the development of tumors, and the expression of  
426 GSDME protein is not always directly related to the volume and weight of tumors, but may  
427 play a key role in tumor immunity and chemotherapy-mediated cell death<sup>44, 45</sup>.

428 GSDME was significantly positively correlated with StromalScore, ImmuneScore and  
429 ESTIMATEScore in tumor microenvironment, and also significantly positively correlated  
430 with Macrophage M1 and T cells CD4 memory activated. GSDME was positively correlated  
431 with TMB in patients with gastric cancer, and negatively correlated with IPS in patients  
432 receiving CTLA4 (+) PD 1 (+), CTLA4 (+) PD 1 (-), CTLA4 (-) PD 1 (+) and CTLA4 (-) PD  
433 1 (-) immunotherapy. These results indicate that GSDME affects the tumor immunity of  
434 gastric cancer, and the high expression of GSDME may indicate that it is difficult for gastric  
435 cancer patients to achieve ideal results in immunotherapy. Although GSDME is difficult to be  
436 used as a diagnostic marker for gastric cancer, it can potentially be used as a marker for  
437 gastric cancer immunotherapy. Recent studies have shown that although GSDME ablation  
438 cannot protect cells from final cell death, its protein expression may still play a role in tumor  
439 immunogenicity, which can induce (secondary) necrotic cell death to enhance  
440 immunogenicity<sup>46</sup>. This provides another evidence for GSDME as an immunotherapy marker.  
441 The increase in immunogenicity after GSDME cleavage may also be why the expression of  
442 GSDME is significantly positively correlated with TMB and the expression of most immune  
443 checkpoint inhibitor genes. For cancer cells with normal expression of GSDME, they showed  
444 CASP3-dependent GSDME activation after chemotherapy treatment<sup>15, 47-49</sup>. The toxicity of  
445 cisplatin on gastric cancer cells decreased after GSDME silencing, which indicated that the  
446 sensitivity of chemotherapeutic drugs was directly related to the expression of GSDME, and  
447 the decrease of GSDME expression affected the efficiency of chemotherapy. Previous studies  
448 have also shown that after GSDME is silenced, A-549 cells induce less cell death due to  
449 cisplatin<sup>48</sup>. The decrease of cisplatin sensitivity in clinical practice may be affected by the  
450 expression of core genes such as GSDME. Some studies have found that knockout of  
451 GSDME transforms platinum-induced cell death from pyroptosis to apoptosis<sup>45</sup>. The results of

452 Western Blot in this study showed that the silencing of GSDME in gastric cancer cells  
453 significantly increased the expression of CASP3 regardless of the effect of cisplatin. This  
454 indicates that CASP3 may mediate the inhibition of GSDME expression. This also indicates  
455 that there is also a CASP3-GSDME mutual regulation / feedback mechanism in gastric cancer  
456 cells<sup>50</sup>. The results showed that the expression of GSDME protein was synergistic with the  
457 expression of Bcl-2 protein in gastric cancer cells. After cisplatin treatment, GSDME protein  
458 and Bcl-2 protein were highly expressed in gastric cancer cells. A decrease in Bcl-2  
459 expression also accompanied the silencing of GSDME. Bcl-2 protein can inhibit the apoptosis  
460 induced by radiotherapy, chemotherapy and other tumor treatments, and the up-regulation of  
461 Bcl-2 is related to the resistance of various cancer cell lines to cisplatin<sup>51, 52</sup>. However, the  
462 expression of Bcl-2 is a good prognostic marker for gastric cancer patients in Asian  
463 countries<sup>53</sup>. The expression of GSDME, an executive protein of pyroptosis, is an unfavorable  
464 factor for the prognosis of gastric cancer patients. Further study on the regulatory system of  
465 GSDME and Bcl-2 is helpful to reveal the mystery of pyroptosis as a 'double-edged sword' for  
466 the occurrence and development of cancer. Chemotherapy drugs including cisplatin have side  
467 effects such as nausea and vomiting, acute kidney injury, neurotoxicity and ototoxicity during  
468 use<sup>54</sup>. Studies have shown that acute kidney injury is significantly related to pyroptosis, and  
469 baicalin can alleviate acute kidney injury by regulating the ROS / NLRP3 / CASP1 / GSDMD  
470 signaling pathway<sup>55</sup>. Currently, most of the studies on ear protection are only achieved by  
471 limiting cisplatin-induced apoptosis. Studies have shown that mutations in GSDME, TJP2 and  
472 MSRB3 can lead to single-gene hearing impairment<sup>56</sup>. Cisplatin may mediate the occurrence  
473 of pyroptosis by activating GSDME, resulting in ototoxicity. The in-depth study of pyroptosis  
474 in ototoxicity and the executive protein GSDME may be conducive to the discovery of more  
475 effective methods for ear protection. The results showed that after cisplatin treatment of  
476 gastric cancer cells, GSDMD and GSDME were significantly up-regulated at the  
477 transcriptome and protein levels. The upregulation of GSDMD protein was significantly  
478 associated with ocular hypertension / glaucoma, lung injury in mice, mastitis in mice, cardiac  
479 hypertrophy, chicken cardiotoxicity and neurotoxicity<sup>57-62</sup>. GSDME, an executive protein  
480 mediated by chemotherapy drugs, is indispensable in killing cancer cells. Without affecting  
481 the expression of GSDME, inhibiting the expression of GSDMD protein seems helpful to  
482 solve the side effects caused by chemotherapy drugs, but further research is needed to clarify  
483 its feasibility. This study is mainly based on cell experiments and has not completed in vivo  
484 experimental verification; no clinical trials have been carried out to further prove the clinical

485 value of GSDME. However, in general, based on various research methods, we have a new  
486 understanding of the mechanism of cisplatin on gastric cancer cells, and also found that  
487 GSDME, a core factor of pyroptosis, has the potential to be a prognostic marker and  
488 immunotherapy marker for gastric cancer.

489 Pyroptosis as an innate immune mechanism mediates the death of tumor cells. On the other  
490 hand, as a way of pro-inflammatory cell death, it may also provide a suitable environment for  
491 tumor growth. In-depth study of the mechanism of pyroptosis and the precise regulation of  
492 pyroptosis are helpful to improve the killing efficiency of cancer cells and reduce the side  
493 effects of drugs.

#### 494 **Conclusion**

495 In this study, we identified that the pyroptosis-related genes were highly expressed after  
496 cisplatin treatment of gastric cancer cells. The pyroptosis core gene GSDME was an  
497 independent prognostic factor for gastric cancer patients. There was no significant difference  
498 in the expression of GSDME between gastric cancer tissues and adjacent tissues. The  
499 silencing of GSDME significantly reduced the sensitivity of AGS cell and MKN45 cell to  
500 cisplatin. The expression of GSDME was significantly negatively correlated with TMB and  
501 IPS after immunotherapy. GSDME can potentially be a biomarker for predicting the  
502 sensitivity of chemotherapy, immunotherapy and prognosis in patients with gastric cancer.

#### 503 **Abbreviation**

504 GSDME: Gasdermin E

505 GSDMD: Gasdermin D

506 IL-6: Interleukin-6

507 CASP1: caspase-1

508 IC50: Half inhibitory concentration

509 TCGA: The Cancer Genome Atlas Program

510 STAD: Stomach adenocarcinoma

511 GO: Gene Ontology

512 KEGG: Kyoto Encyclopedia of Genes and Genomes

513 OS: overall survival

514 FP: free progression

515 PPS: post progression survival

516 IPS: Immunophenoscore

517 Bcl-2: B-Cell CLL/Lymphoma 2



518 CASP3: caspase-3

519 PARP: Poly(ADP-Ribose) Polymerase

520 IL-1 beta: Interleukin-1beta

## 521 **Declarations**

### 522 **Ethics approval and consent to participate**

523 This study was approved by the Medical Ethics Committee of Gansu Provincial People 's

524 Hospital (ID: 2022-316), Lanzhou, China. All patients signed the informed consent and

525 approved the study.

### 526 **Consent for publication**

527 Not applicable

528

### 529 **Data Availability Statement**

530 The datasets analyzed during the current study are available in TCGA

531 (<https://portal.gdc.cancer.gov/>), Gene Expression Profiling Interactive Analysis 2

532 (<http://gepia2.cancer-pku.cn/>), Kaplan Meier plotter portal (<https://kmplot.com/analysis/>),

533 GEO database (<https://www.ncbi.nlm.nih.gov/>), The Molecular Signatures Database

534 (<https://www.gsea-msigdb.org/gsea/msigdb/>), and The Human Protein Atlas

535 (<https://www.proteinatlas.org/>).

### 536 **Competing interests**

537 The authors declare that they have no conflicts of interest to report regarding the present

538 study.

### 539 **Funding**

540 This work was funded by The 2021 Central-Guided Local Science and Technology

541 Development Found (ZYYDDFFZZJ-1); Gansu Key Laboratory of Molecular Diagnosis and

542 Precision Treatment of Surgical Tumors (18JR2RA033); Key Laboratory of Gastrointestinal

543 Cancer Diagnosis and Treatment of National Health Commission (2019PT320005); Key

544 Talent Project of Gansu Province of the Organization Department of Gansu Provincial Party

545 Committee (2020RCXM076); Lanzhou COVID-19 prevention and control technology  
546 research project (2020-XG-1); Lanzhou talent innovation and entrepreneurship Project  
547 (2016-RC-56); Young Science and Technology Talent Support Project of Gansu Association  
548 for Science and Technology (GXH202220530-17) ; The 2022 Master/Doctor/Postdoctoral  
549 program of NHC Key Laboratory of Diagnosis and Therapy of Gastrointestinal Tumor  
550 (NHCDP2022024) and Gansu Provincial Youth Science and Technology Fund Program  
551 (21JR7RA642). The funders had no role in study design, data collection and analysis,  
552 decision to publish, or preparation of the manuscript.

553 **Author Contributions:** Xianglai Jiang and Yongfeng Wang conceived the study, Chenyu  
554 Wang completed the data collation and processing, Miao Yu provided the support of  
555 methodology and Haizhong Ma and Hui Cai completed the work of Funding acquisition.  
556 Xianglai Jiang completed the draft, Hui Cai reviewed the paper.

### 557 **Acknowledgments**

558 This work has benefited from aforementioned databases. The authors thank the Key  
559 Laboratory of Molecular Diagnostics and Precision Medicine for Surgical Oncology in Gansu  
560 Province for their help and support in the methodology.

561

### 562 **References**

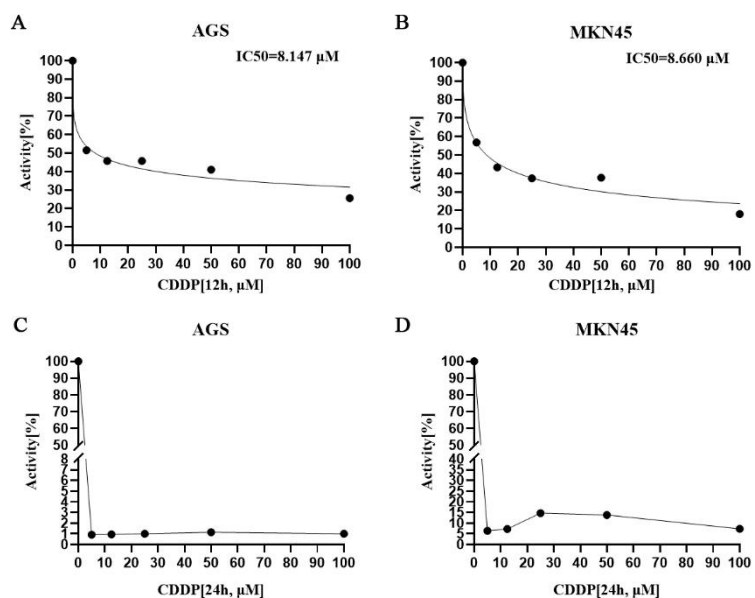
- 563 1. Smyth, E. C.; Nilsson, M.; Grabsch, H. I.; van Grieken, N. C.; Lordick, F., Gastric cancer. *Lancet*  
564 **2020**, *396* (10251), 635-648.
- 565 2. Siegel, R. L.; Miller, K. D.; Wagle, N. S.; Jemal, A., Cancer statistics, 2023. *CA Cancer J Clin* **2023**, *73*  
566 (1), 17-48.
- 567 3. Siegel, R. L.; Miller, K. D.; Fuchs, H. E.; Jemal, A., Cancer Statistics, 2021. *CA Cancer J Clin* **2021**, *71*  
568 (1), 7-33.
- 569 4. Sekiguchi, M.; Oda, I.; Matsuda, T.; Saito, Y., Epidemiological Trends and Future Perspectives of  
570 Gastric Cancer in Eastern Asia. *Digestion* **2022**, *103* (1), 22-28.
- 571 5. Yan, L.; Chen, Y.; Chen, F.; Tao, T.; Hu, Z.; Wang, J.; You, J.; Wong, B. C. Y.; Chen, J.; Ye,

- 572 W., Effect of Helicobacter pylori Eradication on Gastric Cancer Prevention: Updated Report From a  
573 Randomized Controlled Trial With 26.5 Years of Follow-up. *Gastroenterology* **2022**, *163* (1), 154-162.e3.
- 574 6. Wang, J.; Kunzke, T.; Prade, V. M.; Shen, J.; Buck, A.; Feuchtinger, A.; Haffner, I.; Luber, B.;  
575 Liu, D. H. W.; Langer, R.; Lordick, F.; Sun, N.; Walch, A., Spatial Metabolomics Identifies Distinct  
576 Tumor-Specific Subtypes in Gastric Cancer Patients. *Clin Cancer Res* **2022**, *28* (13), 2865-2877.
- 577 7. Douada, L.; Cyrany, J.; Tachecí, I., Early gastric cancer. *Vnitr Lek* **2022**, *68* (6), 371-375.
- 578 8. Li, G. Z.; Doherty, G. M.; Wang, J., Surgical Management of Gastric Cancer: A Review. *JAMA Surg*  
579 **2022**, *157* (5), 446-454.
- 580 9. Zeng, Y.; Jin, R. U., Molecular pathogenesis, targeted therapies, and future perspectives for gastric  
581 cancer. *Semin Cancer Biol* **2022**, *86* (Pt 3), 566-582.
- 582 10. Song, Z.; Wu, Y.; Yang, J.; Yang, D.; Fang, X., Progress in the treatment of advanced gastric  
583 cancer. *Tumour Biol* **2017**, *39* (7), 1010428317714626.
- 584 11. Peng, F.; Liao, M.; Qin, R.; Zhu, S.; Peng, C.; Fu, L.; Chen, Y.; Han, B., Regulated cell death  
585 (RCD) in cancer: key pathways and targeted therapies. *Signal Transduct Target Ther* **2022**, *7* (1), 286.
- 586 12. Elmore, S., Apoptosis: a review of programmed cell death. *Toxicol Pathol* **2007**, *35* (4), 495-516.
- 587 13. Cookson, B. T.; Brennan, M. A., Pro-inflammatory programmed cell death. *Trends Microbiol* **2001**, *9*  
588 (3), 113-4.
- 589 14. Fang, Y.; Tian, S.; Pan, Y.; Li, W.; Wang, Q.; Tang, Y.; Yu, T.; Wu, X.; Shi, Y.; Ma, P.; Shu,  
590 Y., Pyroptosis: A new frontier in cancer. *Biomed Pharmacother* **2020**, *121*, 109595.
- 591 15. Wang, Y.; Gao, W.; Shi, X.; Ding, J.; Liu, W.; He, H.; Wang, K.; Shao, F., Chemotherapy drugs  
592 induce pyroptosis through caspase-3 cleavage of a gasdermin. *Nature* **2017**, *547* (7661), 99-103.
- 593 16. Hsu, S. K.; Li, C. Y.; Lin, I. L.; Syue, W. J.; Chen, Y. F.; Cheng, K. C.; Teng, Y. N.; Lin, Y. H.;  
594 Yen, C. H.; Chiu, C. C., Inflammation-related pyroptosis, a novel programmed cell death pathway, and its  
595 crosstalk with immune therapy in cancer treatment. *Theranostics* **2021**, *11* (18), 8813-8835.
- 596 17. Long, D. F.; Repta, A. J., Cisplatin: chemistry, distribution and biotransformation. *Biopharm Drug*  
597 *Dispos* **1981**, *2* (1), 1-16.
- 598 18. Fuertes, M. A.; Castilla, J.; Alonso, C.; Pérez, J. M., Cisplatin biochemical mechanism of action: from  
599 cytotoxicity to induction of cell death through interconnections between apoptotic and necrotic pathways.  
600 *Curr Med Chem* **2003**, *10* (3), 257-66.
- 601 19. Dasari, S.; Tchounwou, P. B., Cisplatin in cancer therapy: molecular mechanisms of action. *Eur J*  
602 *Pharmacol* **2014**, *740*, 364-78.
- 603 20. Ghosh, S., Cisplatin: The first metal based anticancer drug. *Bioorg Chem* **2019**, *88*, 102925.
- 604 21. Yan, H.; Luo, B.; Wu, X.; Guan, F.; Yu, X.; Zhao, L.; Ke, X.; Wu, J.; Yuan, J., Cisplatin Induces  
605 Pyroptosis via Activation of MEG3/NLRP3/caspase-1/GSDMD Pathway in Triple-Negative Breast Cancer.  
606 *Int J Biol Sci* **2021**, *17* (10), 2606-2621.
- 607 22. Wu, M.; Wang, Y.; Yang, D.; Gong, Y.; Rao, F.; Liu, R.; Danna, Y.; Li, J.; Fan, J.; Chen, J.;  
608 Zhang, W.; Zhan, Q., A PLK1 kinase inhibitor enhances the chemosensitivity of cisplatin by inducing  
609 pyroptosis in oesophageal squamous cell carcinoma. *EBioMedicine* **2019**, *41*, 244-255.
- 610 23. Li, R. Y.; Zheng, Z. Y.; Li, Z. M.; Heng, J. H.; Zheng, Y. Q.; Deng, D. X.; Xu, X. E.; Liao, L. D.;  
611 Lin, W.; Xu, H. Y.; Huang, H. C.; Li, E. M.; Xu, L. Y., Cisplatin-induced pyroptosis is mediated via the  
612 CAPN1/CAPN2-BAK/BAX-caspase-9-caspase-3-GSDME axis in esophageal cancer. *Chem Biol Interact*  
613 **2022**, *361*, 109967.
- 614 24. Tang, Z.; Kang, B.; Li, C.; Chen, T.; Zhang, Z., GEPIA2: an enhanced web server for large-scale

- 615 expression profiling and interactive analysis. *Nucleic Acids Res* **2019**, *47*(W1), W556-w560.
- 616 25. Carlson, M.; Falcon, S.; Pages, H.; Li, N., org. Hs. eg. db: Genome wide annotation for Human. *R*  
617 *package version* **2019**, *3*(2), 3.
- 618 26. Jager, K. J.; Van Dijk, P. C.; Zoccali, C.; Dekker, F. W., The analysis of survival data: the Kaplan–Meier  
619 method. *Kidney international* **2008**, *74*(5), 560–565.
- 620 27. Chan, T. A.; Yarchoan, M.; Jaffee, E.; Swanton, C.; Quezada, S. A.; Stenzinger, A.; Peters, S.,  
621 Development of tumor mutation burden as an immunotherapy biomarker: utility for the oncology clinic.  
622 *Ann Oncol* **2019**, *30*(1), 44–56.
- 623 28. Charoentong, P.; Finotello, F.; Angelova, M.; Mayer, C.; Efremova, M.; Rieder, D.; Hackl, H.;  
624 Trajanoski, Z., Pan-cancer Immunogenomic Analyses Reveal Genotype-Immunophenotype Relationships  
625 and Predictors of Response to Checkpoint Blockade. *Cell Rep* **2017**, *18*(1), 248–262.
- 626 29. D'Souza, C. A.; Heitman, J., Dismantling the Cryptococcus coat. *Trends Microbiol* **2001**, *9*(3), 112–3.
- 627 30. Zhang, C. C.; Li, C. G.; Wang, Y. F.; Xu, L. H.; He, X. H.; Zeng, Q. Z.; Zeng, C. Y.; Mai, F. Y.;  
628 Hu, B.; Ouyang, D. Y., Chemotherapeutic paclitaxel and cisplatin differentially induce pyroptosis in A549  
629 lung cancer cells via caspase-3/GSDME activation. *Apoptosis* **2019**, *24*(3–4), 312–325.
- 630 31. Gorman, A. M., Neuronal cell death in neurodegenerative diseases: recurring themes around protein  
631 handling. *J Cell Mol Med* **2008**, *12*(6a), 2263–80.
- 632 32. Moujalled, D.; Strasser, A.; Liddell, J. R., Molecular mechanisms of cell death in neurological diseases.  
633 *Cell Death Differ* **2021**, *28*(7), 2029–2044.
- 634 33. Zhao, N.; Sun, C.; Zheng, M.; Liu, S.; Shi, R., Amentoflavone suppresses amyloid  $\beta$ 1–42  
635 neurotoxicity in Alzheimer's disease through the inhibition of pyroptosis. *Life Sci* **2019**, *239*, 117043.
- 636 34. Cai, Y.; Chai, Y.; Fu, Y.; Wang, Y.; Zhang, Y.; Zhang, X.; Zhu, L.; Miao, M.; Yan, T., Salidroside  
637 Ameliorates Alzheimer's Disease by Targeting NLRP3 Inflammasome-Mediated Pyroptosis. *Front Aging*  
638 *Neurosci* **2021**, *13*, 809433.
- 639 35. Zhang, X.; Zhang, Y.; Li, R.; Zhu, L.; Fu, B.; Yan, T., Salidroside ameliorates Parkinson's disease by  
640 inhibiting NLRP3-dependent pyroptosis. *Aging (Albany NY)* **2020**, *12*(10), 9405–9426.
- 641 36. Hermansson, A. K.; Paciello, I.; Bernardini, M. L., The Orchestra and Its Maestro: Shigella's  
642 Fine-Tuning of the Inflammasome Platforms. *Curr Top Microbiol Immunol* **2016**, *397*, 91–115.
- 643 37. Yu, X.; He, S., GSDME as an executioner of chemotherapy-induced cell death. *Sci China Life Sci* **2017**,  
644 *60*(11), 1291–1294.
- 645 38. Liang, C.; Fan, J.; Liang, C.; Guo, J., Identification and Validation of a Pyroptosis-Related Prognostic  
646 Model for Gastric Cancer. *Front Genet* **2021**, *12*, 699503.
- 647 39. Wang, Z.; Cao, L.; Zhou, S.; Lyu, J.; Gao, Y.; Yang, R., Construction and Validation of a Novel  
648 Pyroptosis-Related Four-lncRNA Prognostic Signature Related to Gastric Cancer and Immune Infiltration.  
649 *Front Immunol* **2022**, *13*, 854785.
- 650 40. Wang, Y.; Chen, X.; Jiang, F.; Shen, Y.; Fang, F.; Li, Q.; Yang, C.; Dong, Y.; Shen, X., A  
651 prognostic signature of pyroptosis-related lncRNAs verified in gastric cancer samples to predict the  
652 immunotherapy and chemotherapy drug sensitivity. *Front Genet* **2022**, *13*, 939439.
- 653 41. Guan, S. H.; Wang, X. Y.; Shang, P.; Du, Q. C.; Li, M. Z.; Xing, X.; Yan, B., Pyroptosis-related  
654 genes play a significant role in the prognosis of gastric cancer. *World J Clin Cases* **2022**, *10*(24),  
655 8490–8505.
- 656 42. Wei, X.; Xie, F.; Zhou, X.; Wu, Y.; Yan, H.; Liu, T.; Huang, J.; Wang, F.; Zhou, F.; Zhang, L.,  
657 Role of pyroptosis in inflammation and cancer. *Cell Mol Immunol* **2022**, *19*(9), 971–992.

- 658 43. Yu, P.; Zhang, X.; Liu, N.; Tang, L.; Peng, C.; Chen, X., Pyroptosis: mechanisms and diseases.  
659 *Signal Transduct Target Ther* **2021**, *6* (1), 128.
- 660 44. Lu, H.; Zhang, S.; Wu, J.; Chen, M.; Cai, M. C.; Fu, Y.; Li, W.; Wang, J.; Zhao, X.; Yu, Z.;  
661 Ma, P.; Zhuang, G., Molecular Targeted Therapies Elicit Concurrent Apoptotic and GSDME-Dependent  
662 Pyroptotic Tumor Cell Death. *Clin Cancer Res* **2018**, *24* (23), 6066-6077.
- 663 45. Yu, J.; Li, S.; Qi, J.; Chen, Z.; Wu, Y.; Guo, J.; Wang, K.; Sun, X.; Zheng, J., Cleavage of  
664 GSDME by caspase-3 determines lobaplatin-induced pyroptosis in colon cancer cells. *Cell Death Dis* **2019**,  
665 *10* (3), 193.
- 666 46. De Schutter, E.; Croes, L.; Ibrahim, J.; Pauwels, P.; Op de Beeck, K.; Vandenaabeele, P.; Van  
667 Camp, G., GSDME and its role in cancer: From behind the scenes to the front of the stage. *Int J Cancer*  
668 **2021**, *148* (12), 2872-2883.
- 669 47. Lage, H.; Helmbach, H.; Grottke, C.; Dietel, M.; Schadendorf, D., DFNA5 (ICERE-1) contributes to  
670 acquired etoposide resistance in melanoma cells. *FEBS Lett* **2001**, *494* (1-2), 54-9.
- 671 48. Zhang, J.; Chen, Y.; He, Q., Distinct characteristics of dasatinib-induced pyroptosis in gasdermin  
672 E-expressing human lung cancer A549 cells and neuroblastoma SH-SY5Y cells. *Oncol Lett* **2020**, *20* (1),  
673 145-154.
- 674 49. Deng, B. B.; Jiao, B. P.; Liu, Y. J.; Li, Y. R.; Wang, G. J., BIX-01294 enhanced chemotherapy effect in  
675 gastric cancer by inducing GSDME-mediated pyroptosis. *Cell Biol Int* **2020**, *44* (9), 1890-1899.
- 676 50. Jiang, M.; Qi, L.; Li, L.; Li, Y., The caspase-3/GSDME signal pathway as a switch between apoptosis  
677 and pyroptosis in cancer. *Cell Death Discov* **2020**, *6*, 112.
- 678 51. Low, S. Y.; Tan, B. S.; Choo, H. L.; Tiong, K. H.; Khoo, A. S.; Leong, C. O., Suppression of BCL-2  
679 synergizes cisplatin sensitivity in nasopharyngeal carcinoma cells. *Cancer Lett* **2012**, *314* (2), 166-75.
- 680 52. Yang, M.; Yang, X. M.; Yin, D. H.; Tang, Q. L.; Wang, L.; Huang, C.; Li, P.; Li, S. S., Beclin1  
681 enhances cisplatin-induced apoptosis via Bcl-2-modulated autophagy in laryngeal carcinoma cells Hep-2.  
682 *Neoplasma* **2018**, *65* (1), 42-48.
- 683 53. Cheng, H.; Wang, X.; Li, T.; Chen, L., Bcl-2 expression and patient survival in gastric cancer: a  
684 systematic review of the literature with meta-analysis. *Med Oncol* **2015**, *32* (1), 389.
- 685 54. Desilets, A.; Adam, J. P.; Soulières, D., Management of cisplatin-associated toxicities in bladder  
686 cancer patients. *Curr Opin Support Palliat Care* **2020**, *14* (3), 286-292.
- 687 55. Li, Y.; Wang, J.; Huang, D.; Yu, C., Baicalin Alleviates Contrast-Induced Acute Kidney Injury Through  
688 ROS/NLRP3/Caspase-1/GSDMD Pathway-Mediated Proptosis in vitro. *Drug Des Devel Ther* **2022**, *16*,  
689 3353-3364.
- 690 56. Op de Beeck, K.; Schacht, J.; Van Camp, G., Apoptosis in acquired and genetic hearing impairment:  
691 the programmed death of the hair cell. *Hear Res* **2011**, *281* (1-2), 18-27.
- 692 57. Han, X.; Xu, T.; Fang, Q.; Zhang, H.; Yue, L.; Hu, G.; Sun, L., Quercetin hinders microglial  
693 activation to alleviate neurotoxicity via the interplay between NLRP3 inflammasome and mitophagy. *Redox*  
694 *Biol* **2021**, *44*, 102010.
- 695 58. Zhang, Y.; Yin, K.; Wang, D.; Wang, Y.; Lu, H.; Zhao, H.; Xing, M., Polystyrene  
696 microplastics-induced cardiotoxicity in chickens via the ROS-driven NF- $\kappa$ B-NLRP3-GSDMD and  
697 AMPK-PGC-1 $\alpha$  axes. *Sci Total Environ* **2022**, *840*, 156727.
- 698 59. Wang, F.; Liang, Q.; Ma, Y.; Sun, M.; Li, T.; Lin, L.; Sun, Z.; Duan, J., Silica nanoparticles induce  
699 pyroptosis and cardiac hypertrophy via ROS/NLRP3/Caspase-1 pathway. *Free Radic Biol Med* **2022**, *182*,  
700 171-181.

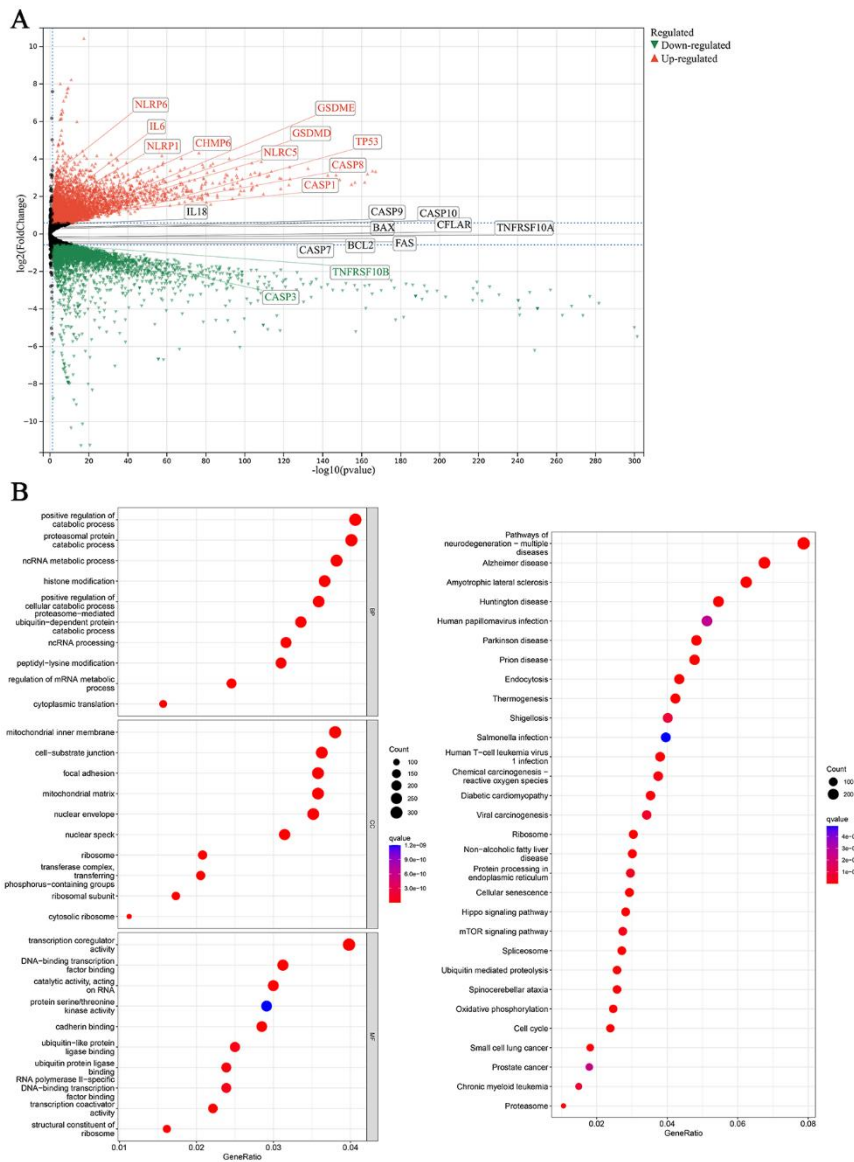
701 60. Li, L.; Xing, C.; Zhou, J.; Niu, L.; Luo, B.; Song, M.; Niu, J.; Ruan, Y.; Sun, X.; Lei, Y.,  
702 Airborne particulate matter (PM(2.5)) triggers ocular hypertension and glaucoma through pyroptosis. *Part*  
703 *Fibre Toxicol* **2021**, *18* (1), 10.  
704 61. Ran, X.; Yan, Z.; Yang, Y.; Hu, G.; Liu, J.; Hou, S.; Guo, W.; Kan, X.; Fu, S., Dioscin Improves  
705 Pyroptosis in LPS-Induced Mice Mastitis by Activating AMPK/Nrf2 and Inhibiting the NF- $\kappa$ B Signaling  
706 Pathway. *Oxid Med Cell Longev* **2020**, *2020*, 8845521.  
707 62. Xiong, R.; Jiang, W.; Li, N.; Liu, B.; He, R.; Wang, B.; Geng, Q., PM2.5-induced lung injury is  
708 attenuated in macrophage-specific NLRP3 deficient mice. *Ecotoxicol Environ Saf* **2021**, *221*, 112433.  
709



710

711 **Figure 1:** The cell viability curves of AGS cells (A) and MKN45 cells (B) co-cultured with  
712 IC50 concentration of cisplatin for 12 hours, and the cell viability curves of AGS cells (C) and  
713 MKN45 cells (D) cultured with IC50 concentration of cisplatin for 24 hours.

714



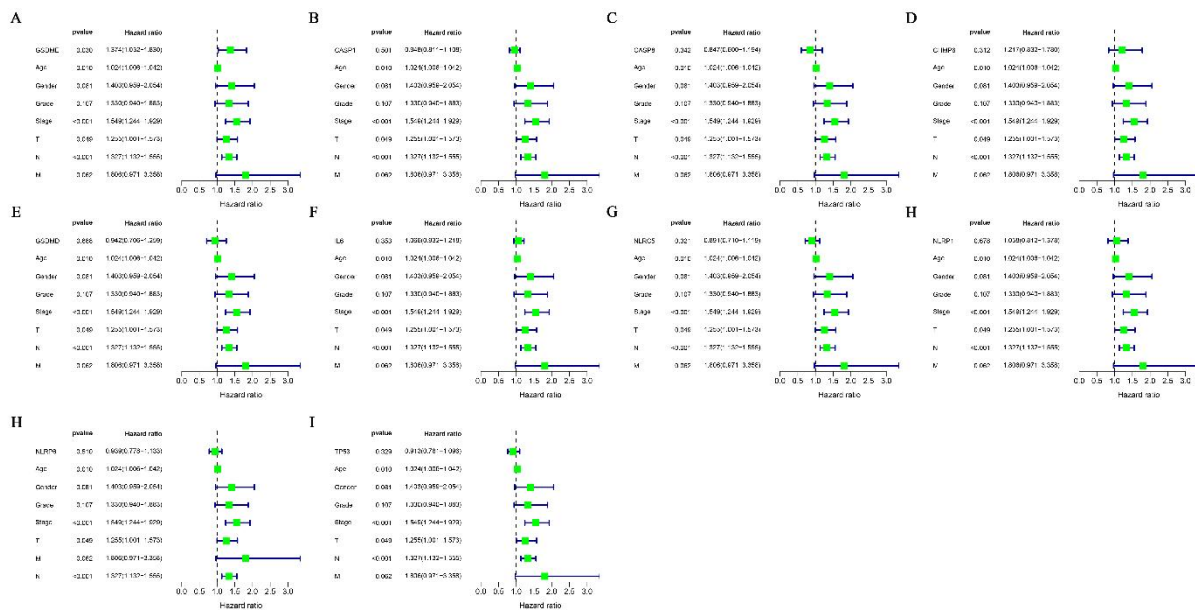
715

716 **Figure 2:** Volcano map based on differential genes after cisplatin treatment of MKN45 cells

717 for 12 hours (A); after 12 hours of cisplatin treatment of MKN45 cells, GO enrichment

718 analysis and KEGG enrichment analysis based on differential genes (B).

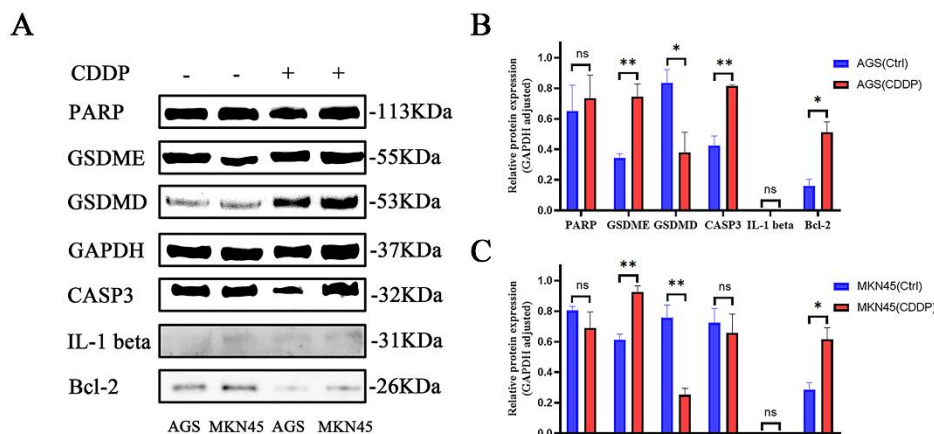
719



720

721 **Figure 3:** Single factor Cox regression analysis of pyroptosis core genes GSDME (A),  
722 CASP1 (B), CASP8 (C), CHMP6 (D), GSDMD (E), IL6 (F), NLRC5 (G), NLRP1 (H),  
723 NLRP6 (I) and TP53 (J) highly expressed in gastric cancer cells after cisplatin treatment.

724

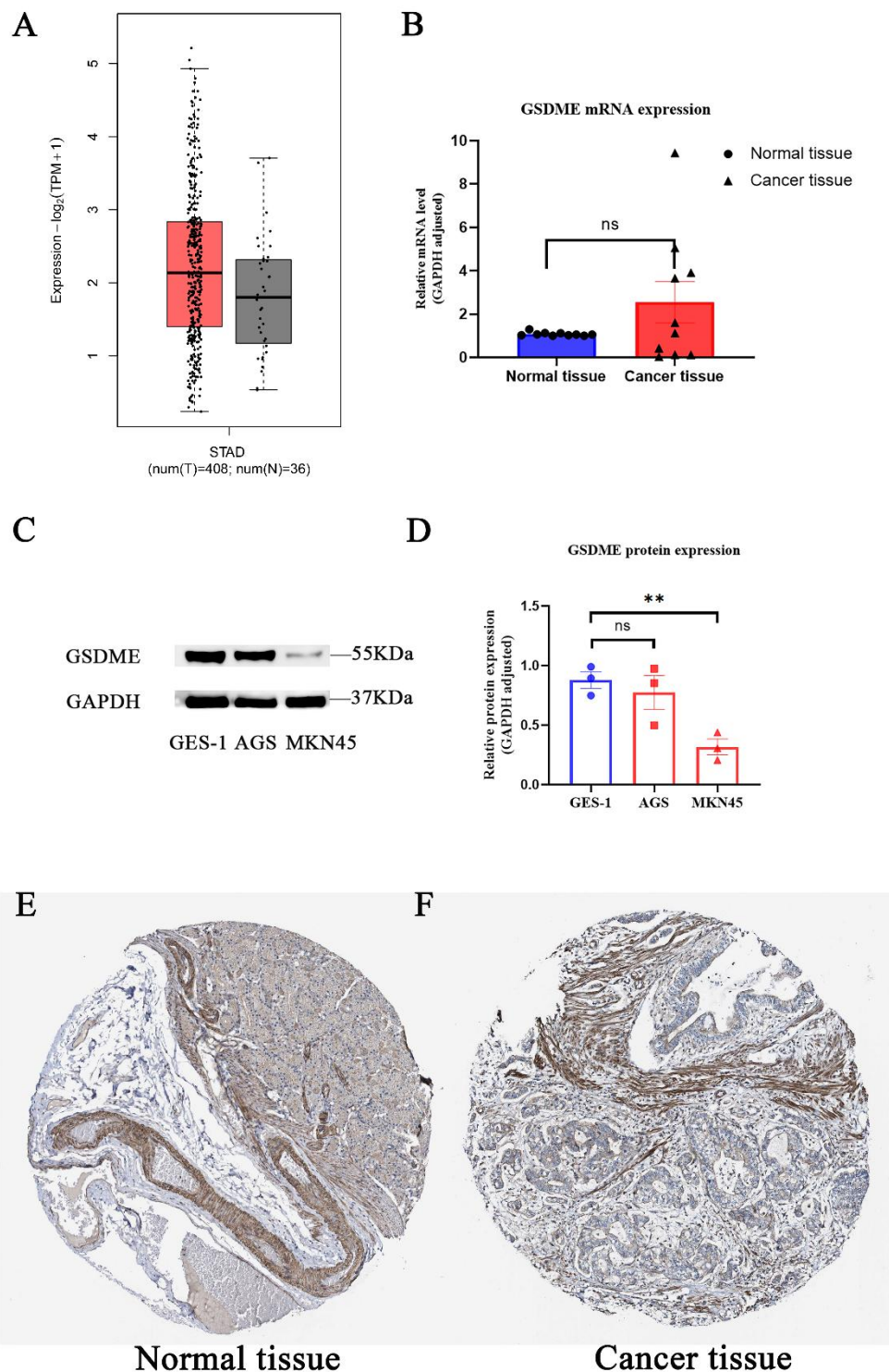


725

726 **Figure 4:** The changes of PARP, GSDME, GSDMD, GAPDH, CASP3, IL-1 beta, and Bcl-2  
727 protein in gastric cancer cells after cisplatin treatment (A), and the statistical calculation  
728 results of expression in AGS cells (B) and MKN45 (C) cells, respectively.



729

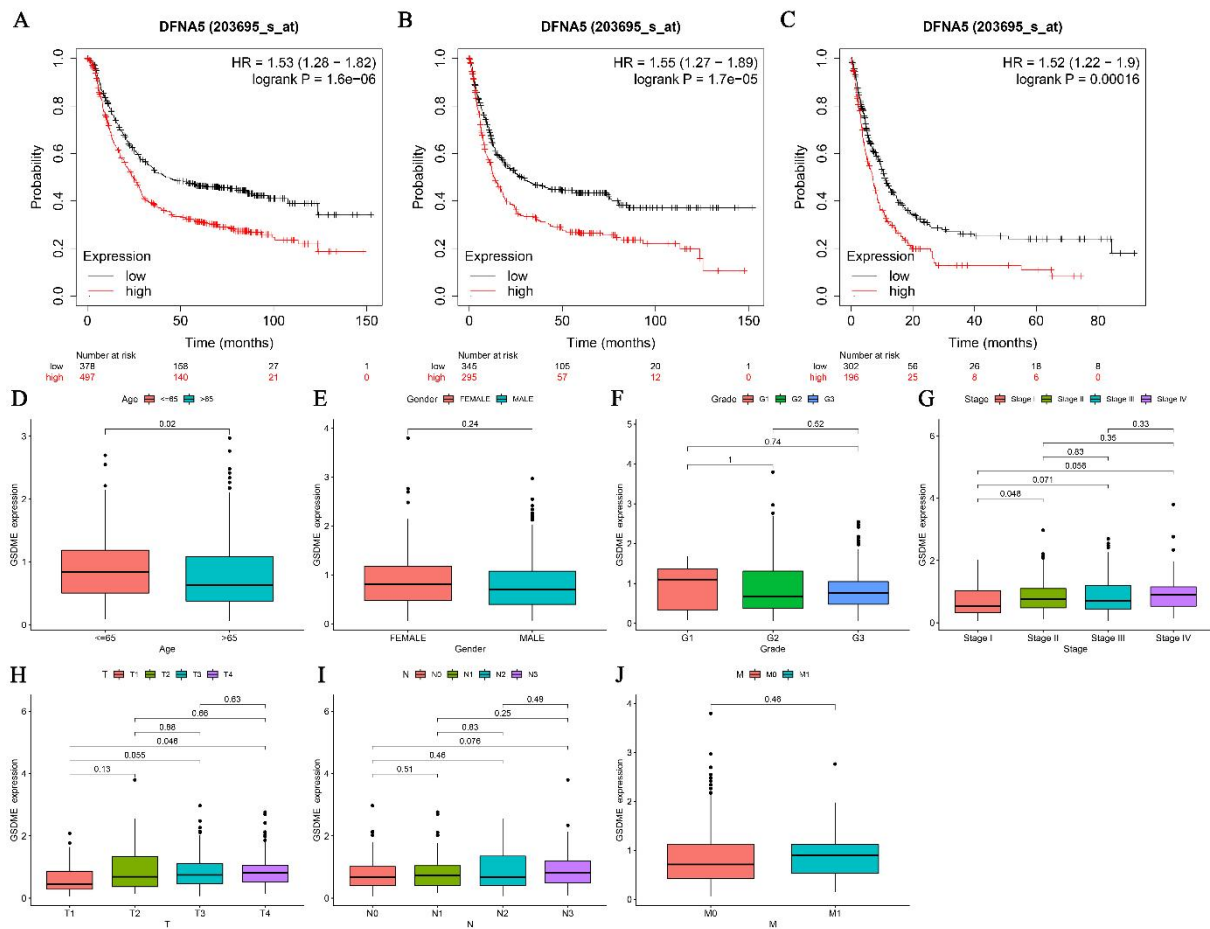


730

731 **Figure 5:** Differential expression of GSDME mRNA in gastric cancer tissues and adjacent

732 tissues from TCGA database (A) and gastric cancer tissues (B); differential expression of

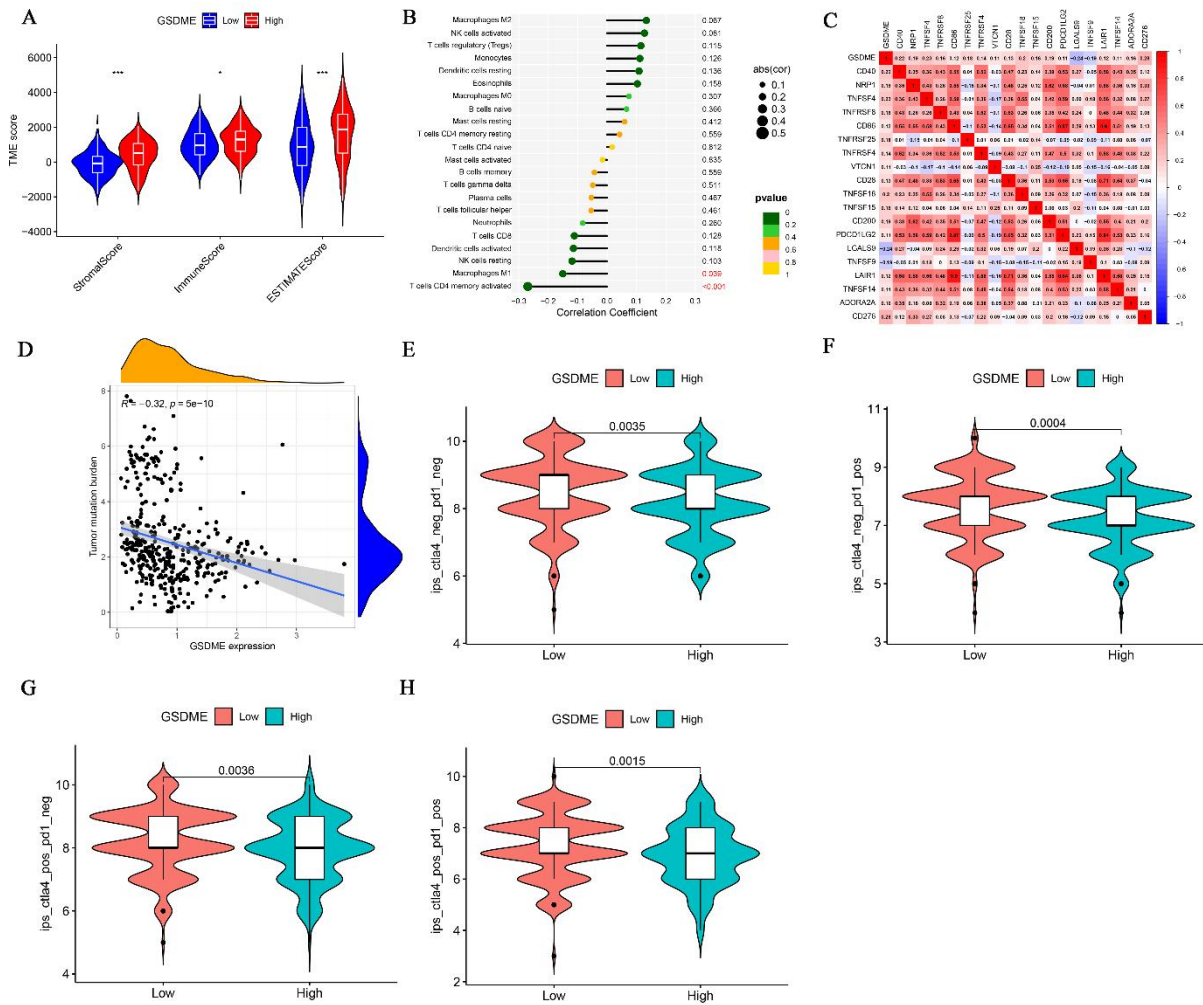
733 GSDME protein between gastric cancer cells and normal gastric epithelial cells (C) and  
 734 statistical calculation results (D); the expression of GSDME protein in normal gastric tissue  
 735 (E) and gastric cancer tissue (F) was from HPA database.  
 736



737

738 **Figure 6:** Correlation between GSDME expression and overall survival (A), progression-free  
 739 survival (B) and post-progression survival (C) in patients with gastric cancer; the expression  
 740 of GSDME in different age (D), gender (E), grade (F), stage (G), T stage (H), N stage (I) and  
 741 M stage (J) of gastric cancer patients.

742



743

744 **Figure 7:** Correlation between GSDME expression and StromalScore, ImmuneScore, and

745 ESTIMATEScore in tumor microenvironment (A), and correlation between GSDME and

746 immune cell infiltration (B); the correlation between GSDME expression and immune

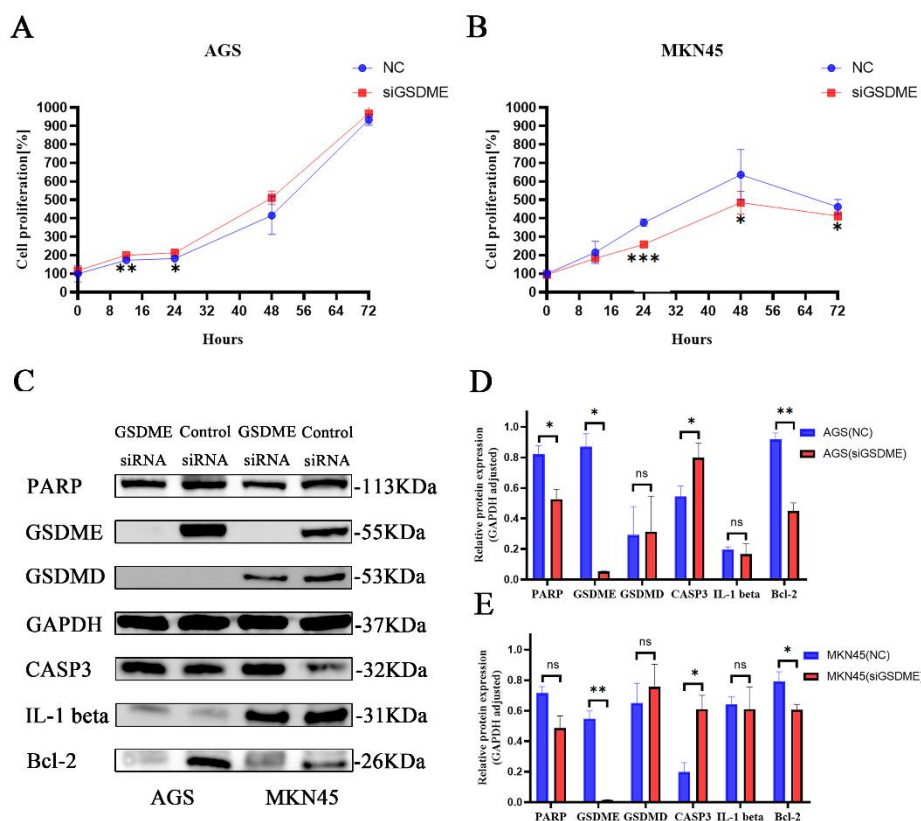
747 checkpoint inhibitor gene expression in gastric cancer (C); the expression of GSDME in

748 gastric cancer was correlated with tumor mutation burden (D); the correlation between

749 GSDME expression in gastric cancer and IPS(F-H) treated with CTLA4 (-) PD1 (-), CTLA4

750 (-) PD1 (+), CTLA4 (+) PD1 (-) and CTLA4 (+) PD1 (+).

751



752

753 **Figure 8:** Changes in the proliferation of AGS cells (A) and MKN45 (B) cells after silencing

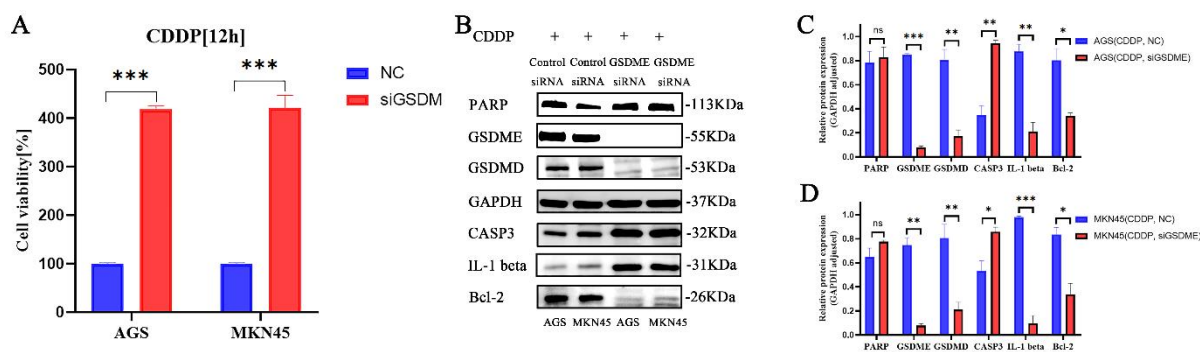
754 the expression of GSDME by siRNA; the changes of PARP, GSDME, GSDMD, GAPDH, CASP3, IL-1

755 beta, and Bcl-2 proteins after silencing the expression of GSDME by siRNA (C), and the

756 difference analysis results in AGS cells (D) and MKN45 cells (E).

757

758



759

760 **Figure 9:** Changes in cell viability (A), PARP, GSDMD, GAPDH, CASP3, IL-1 beta, and  
761 Bcl-2 proteins in gastric cancer cells treated with cisplatin after silencing GSDME by siRNA  
762 (B) and the calculation results in AGS cells (C) and MKN45 (D) cells.  
763